Role of permanent dipoles and orientational averaging in the phase control of two-color, simultaneous one- and three-photon molecular excitations

Alex Brown and William J. Meath
Department of Chemistry and Centre for Interdisciplinary Studies in Chemical Physics, University of Western Ontario, London, Ontario, Canada N6A 5B7
(Received 25 September 1995)

The effects of permanent dipole moments and those due to the randomness of molecular orientation in the phase control of molecular excitation are discussed for the simultaneous one- and three-photon excitation of a two-level model molecule. In this transition scheme both transitions can occur with or without the presence of permanent dipoles and the results are contrasted to those corresponding to the one- and two-photon excitation of a two-level molecule, which requires the presence of permanent dipoles. The dependence of the temporal evolution of the excited state and the associated resonance profiles on the relative phase of the lasers is used to monitor the control of the excitation process. Analytical perturbation theory, the rotating-wave approximation, and exact Floquet results for those observables are used for this purpose. Both fixed molecule-laser configurations and situations where the absorbing molecules assume random orientations with respect to the laser beams are considered.

PACS number(s): 33.80.Wz

I. INTRODUCTION

The effects of a nonzero difference $\mathbf{d}$, between the permanent dipole moments of the states involved in a transition, on the dynamics, and the resonance profiles, associated with the interaction of either one or two continuous wave (cw) or pulsed lasers with a molecule can be significant; see for example [1–11], and references therein. Many of the investigations of the effects of permanent dipoles have involved using analytical rotating-wave approximations (RWA's) and exact Floquet techniques, as well as other methods. In general, for two-color (i.e., two-laser) excitation of a two-level model molecule, the analytical RWA results [4] for the time-dependent and steady-state populations of the molecular states are applicable only when one two-color resonance dominates the transition of interest [4]. Recently an extension of the original two-color RWA to the harmonic two-color excitation problem, where the frequencies of the two lasers are integer multiples of another frequency, has been developed [10]. It is generally applicable to two-level, harmonic two-color, excitation problems, including the important case of competing resonances, and has been used [10] to help investigate the control of molecular two-color excitation, through the interplay between competing one- and two-photon resonances, by variation of the relative phase of the two lasers; both fixed molecule-laser configurations and the effects of orientational averaging were considered in some detail. The effects of $\mathbf{d}\neq\mathbf{0}$ are crucial in this case since for two (nondegenerate) levels the two-photon transition is forbidden unless $\mathbf{d}\neq\mathbf{0}$ [1–7,9–11].

The purpose of this paper is to further investigate the effects of permanent dipole moments and those due to randomness of molecular orientation with respect to the laser beams, in the phase control [12–19] of molecular excitation, by examining a two-level excitation scheme, in this case simultaneous one- and three-photon excitation, where both transitions can occur both with ($\mathbf{d}\neq\mathbf{0}$) and without ($\mathbf{d}=\mathbf{0}$) the presence of permanent dipole moments. Indeed the three-photon transition can depend markedly on the relative size of the transition dipole μ relative to $\mathbf{d}$ [7]. Both the temporal evolution of the population of the states of the two-level dipolar model molecule and the associated resonance profiles are considered.

The methods used to study the problem, namely, the recently developed harmonic many-resonance rotating-wave approximation (HMR RWA) [10], semiclassical time-dependent perturbation theory [6,7,11,20], and exact Floquet methods [2,4,21–25], are discussed briefly in Sec. II. The perturbative results are valid for short times, such that the excited state of the system is far from saturation, and can provide considerable insight into the phase control problem. The HMR RWA is generally more appropriate for longer times and for discussing resonance profiles, and also gives physical insight due to the analytical nature of the RWA expressions for the time-dependent populations of the molecular states and for the resonance profiles. Both perturbation theory and the HMR RWA can be used to estimate the field strengths needed for optimal control of the two-color transition and their validity is tested using exact Floquet results. Interestingly, the perturbative results for the required molecule–electromagnetic-field (EMF) couplings for the three-photon transition are generally considerably more reliable than the RWA couplings.

The effects of the presence of permanent dipole moments on the phase control of the two-color excitation process are discussed in Secs. III A–III D for a fixed molecule-EMF configuration corresponding to $\boldsymbol{\mu}\|\mathbf{d}$ and also parallel to the two polarization vectors of the two cw lasers. Model two-level molecules are used for this purpose that vary from each other by the choice of d relative to μ. Comparisons between simultaneous three- and one-photon excitation, with and without permanent dipoles, are made as a function of relative laser phase using perturbation theory for $\mathbf{d}=\mathbf{0}$ and both perturbation theory and the HMR RWA for $\mathbf{d}\neq\mathbf{0}$ to estimate the field strengths needed for optimal control; the validity of the

HMR RWA for the three-photon molecule-EMF coupling decreases markedly as $(d/\mu)\rightarrow 0$. The effects of taking account of the randomness of molecular orientation with respect to the polarization directions of the lasers on these results are discussed in Sec. III E. Section III includes a discussion of the model calculations in the light of the phase control of the temporal evolution of the molecular states and the effects of phase on the related resonance profiles as a function of $\boldsymbol{\mu}$, $\mathbf{d}$, and the method used to select the optimal control laser field strengths. The presence of permanent dipoles must be taken into account when choosing the laser fields for optimal control; otherwise the phase dependence of the dynamics and the resonance profiles will be largely lost. The results for the one- and three-photon competition are contrasted with the recent work [10] involving the phase control of the simultaneous one- and two-photon excitation of dipolar molecules. In both cases the results are very phase dependent, for the proper choice of the laser fields, for fixed molecule-EMF configurations, while upon orientational averaging the phase dependence is largely lost (more so for the one- and two-photon competition). Some of the more relevant aspects of this work, including a discussion of some of the more general implications of the results for the phase control of molecular excitation, are summarized in Sec. IV.

Atomic units are often used in this paper. The units for energy E, the transition and permanent dipole moments μ_{jk}, the field frequencies ω_j, time t, and the field strengths $\boldsymbol{\varepsilon}_j^0$ are E_H, ea_0, $E_H\hbar^{-1}$, $\hbar E_H^{-1}$, and $E_H(ea_0)^{-1}$, respectively, where E_H is the Hartree of energy, e is the absolute value of the charge of an electron, a_0 is the Bohr radius, and $\hbar$ is the reduced Planck constant. The following conversion factors will be useful in what follows: $ea_0\approx 2.5415$ D, $E_H\hbar^{-1}\approx 4.556\times 10^{-6}$ cm^{-1}, $\hbar E_H^{-1}\approx 2.4189\times 10^{-17}$ s (10^{12} ps=s), and the field intensity corresponding to a continuous-wave electric field is $I\approx 3.509\times 10^{16}$ $(\boldsymbol{\varepsilon}^{(0)}$ au$)^2$ W/cm^2.

II. CALCULATIONAL METHODS

In the semiclassical electric-dipole approximation, the time-dependent Schrödinger wave equation for the interaction of an N-level molecule with a sinusoidal electromagnetic field is given in matrix form by

$$i\frac{\partial \mathbf{a}(t)}{\partial t}=[\mathbf{E}-\boldsymbol{\mu}\cdot\boldsymbol{\varepsilon}(t)]\mathbf{a}(t). \tag{1}$$

The square energy and dipole moment matrices are defined by $(\mathbf{E})_{jk}=E_j\delta_{jk}$ and $(\boldsymbol{\mu})_{jk}=\langle\psi_j|\boldsymbol{\mu}|\psi_k\rangle$, where $\boldsymbol{\mu}$ is the dipole moment operator for the molecule. The $\psi_j(r)$ are the orthonormalized time-independent wave functions for the stationary states having energy E_j and the time-dependent state amplitudes $a_j(t)$ are contained in the column vector $\mathbf{a}(t)$ defined by $[\mathbf{a}(t)]_j=a_j(t)$. For the interaction involving two linearly polarized continuous wave lasers, the electric field is

$$\boldsymbol{\varepsilon}(t)=\hat{\mathbf{e}}_1\varepsilon_1^0\cos(\omega_1 t+\delta_1)+\hat{\mathbf{e}}_3\varepsilon_3^0\cos(\omega_3 t+\delta_3), \tag{2}$$

where $\hat{\mathbf{e}}_i$, ε_i^0, ω_i, and δ_i are, respectively, the polarization unit vector, field strength, circular frequency, and phase of the ith cw electric field. The convention $(i=1,3)$ is chosen since the problem of interest involves the simultaneous one-photon and three-photon absorption for a two-level molecule, i.e., $(E_{21}=E_2-E_1>0)\sim\omega_1\sim 3\omega_3$.

For two independent frequencies, the electric field is periodic in $2\pi/\omega_b$, where ω_b, the beat frequency, is given by [4,26]

$$\omega_b=\frac{\omega_1}{m_1}=\frac{\omega_3}{m_3} \tag{3}$$

and m_1 and m_3 are the lowest possible integers giving the frequency ratio ω_3/ω_1. However, for the laser-molecule interaction involving the fundamental and its third harmonic, i.e., the case considered here, the two frequencies involved are not mutually independent but rather are harmonics of the beat frequency and m_1 and m_3 are positive integers that specify the harmonic relationship between ω_1 and ω_3, i.e., $m_1=3$ and $m_3=1$. The fundamental frequency is denoted by the subscript 3, while its third harmonic is denoted by the subscript 1; $\omega_b=\omega_3$.

A. Perturbation theory ($\mu_{ii}\neq 0$)

Following the standard procedures of semiclassical perturbation theory [7,20], the time-dependent wave function for the two-level molecule is transformed to an interaction representation and written as

$$\Psi=\sum_{j=1}^{2} b_j(t)\psi_j\exp(-iE_j t/\hbar). \tag{4}$$

The time-dependent coefficients $b_j(t)$ can then be expanded perturbatively to obtain [7,20]

$$b_j(t)=\sum_{n=0}^{\infty} b_j^{(n)}(t). \tag{5}$$

The $b_j^{(n)}(t)$ satisfy the coupled differential equations given by

$$\frac{d}{dt}b_j^{(n)}(t)=-\frac{i}{\hbar}\sum_{k=1}^{2}\boldsymbol{\mu}_{jk}\cdot\boldsymbol{\varepsilon}(t)b_k^{(n-1)}\exp\left[\frac{i}{\hbar}(E_j-E_k)t\right]. \tag{6}$$

For initial conditions $b_j(0)=\delta_{j1}$, corresponding to the molecule being in the ground state at time $t=0$, a third-order perturbation treatment of the problem, which neglects the off-resonance terms, yields results similar to the independent one- and three-photon one-color work [7], except for an important interference term. Here the one-photon perturbative molecule-EMF coupling $[C(1)]_{\text{pert}}$ is given by

$$[C(1)]_{\text{pert}}=(\varepsilon_1^0)(\boldsymbol{\mu}\cdot\hat{\mathbf{e}}_1). \tag{7}$$

The three-photon perturbative molecule-EMF coupling $[C(3)]_{\text{pert}}$ is [7]

$$[C(3)]_{\text{pert}}=\frac{(\varepsilon_3^0/2)^3}{2\omega_b^2}[2(\mathbf{d}\cdot\hat{\mathbf{e}}_3)^2-(\boldsymbol{\mu}\cdot\hat{\mathbf{e}}_3)^2](\boldsymbol{\mu}\cdot\hat{\mathbf{e}}_3), \tag{8}$$

where $\mathbf{d}=\boldsymbol{\mu}_{22}-\boldsymbol{\mu}_{11}$, the difference between the permanent dipoles of the excited and ground molecular states. The perturbative expression for the time-dependent population of the excited state 2 is given by

$$P_2(\delta_1,\delta_3,t)=\frac{t^2}{4}\{[C(1)]^2_{\rm pert}+[C(3)]^2_{\rm pert} +2[C(1)]_{\rm pert}[C(3)]_{\rm pert}\cos\delta\}, \quad (9)$$

where the relative phase $\delta=\delta_1-3\delta_3$. This expression neglects small molecule-EMF coupling terms, varying as $(\varepsilon_1^0)^3$ and $\varepsilon_1(\varepsilon_3^0)^2$, and has the form usually associated with competitive one- versus three-photon transitions [13,14,16–19]. However, perturbation theory is only valid for weak perturbations (weak molecule-EMF couplings) and for short times so the excited state is far from saturation. On the other hand, RWA's can give closed-form analytical expressions for both temporal and long-time averaged (resonance profiles) results for the populations of the molecular states that are often valid under much less restrictive conditions (see Sec. II B).

B. Harmonic many-resonance rotating-wave approximation ($\boldsymbol{\mu}_{ii}\neq\mathbf{0}$)

Previously Kondo, Blokker, and Meath [4] have derived analytical expressions, in the RWA, for the resonance profiles and the underlying temporal behavior of the molecular states, associated with the two-color excitation of the two-level dipolar molecule. This approximate solution is not applicable when there are significant competing resonances [4], except when a transition is exactly on resonance [4,27]. More recently Brown and Meath [10] showed, for the more specialized case when the frequencies of the two cw fields involved in the two-color excitation process are both harmonics of another frequency, that the two-color problem can be reduced to an effective one-color problem. In this HMR RWA, analytical results for the time-dependent populations of the molecular states and for the associated resonance profiles are available that are applicable in the case of competing resonances and for both on- and off-resonance frequencies. A detailed derivation of the harmonic many-resonance RWA for the interaction of two continuous wave lasers with a two-level molecule, including the effects of μ_{ii}, is given elsewhere; the relevant equations are given below.

The HMR-RWA expression for the phase-dependent time-dependent population of excited state 2, subject to the initial conditions $\mathbf{a}_1(0)=1$ and $\mathbf{a}_2(0)=0$, is

$$P_2(\delta_1,\delta_3,t)=2\bar{P}_2(\delta_1,\delta_3)\sin^2\{\tfrac{1}{2}[|\zeta(\delta_1,\delta_3)|^2+\Delta^2]^{1/2}t\}, \quad (10)$$

where $\bar{P}_2(\delta_1,\delta_3)$ is the phase-dependent long-time averaged (steady-state) excited-state population

$$\bar{P}_2(\delta_1,\delta_3)=\frac{|\zeta(\delta_1,\delta_3)|^2}{2[|\zeta(\delta_1,\delta_3)|^2+\Delta^2]} \quad (11)$$

and Δ is the detuning of the two fields from the weak-field resonance position

$$\Delta=E_{21}-N_1\omega_1-N_3\omega_3=E_{21}-N_b\omega_b, \quad (12)$$

where ω_b is the beat frequency defined by Eq. (3) and $N_b=N_1m_1+N_3m_3$. Unlike the one-color RWA [1], where there is only one resonance condition $E_{21}=N\omega$, there are an (infinite) number of frequency combinations that satisfy the resonance condition ($\Delta=0$) in the two-color RWA [4], where N_1 and N_3 are integers that can be positive, negative, or one of them zero.

For the harmonic (N_1,N_3)-photon transitions defined by Eqs. (3) and (12), where ω_1 and ω_3 are such that m_1 and m_3 have fixed values, the overall phase-dependent molecule-EMF coupling $\zeta(\delta_1,\delta_3)$ is given by [4]

$$\zeta(\delta_1,\delta_3)=\sum_{N_1,N_3}C(N_1,N_3)\exp[i(N_1\delta_1+N_3\delta_3)], \quad (13)$$

where the molecule-EMF coupling for the individual (N_1,N_3)-photon transition is

$$C(N_1,N_3)=2J_{N_1}(z_1)J_{N_3}(z_3)\left[N_1\omega_1\left(\frac{\boldsymbol{\mu}\cdot\hat{\mathbf{e}}_1}{\mathbf{d}\cdot\hat{\mathbf{e}}_1}\right)+N_3\omega_3\left(\frac{\boldsymbol{\mu}\cdot\hat{\mathbf{e}}_3}{\mathbf{d}\cdot\hat{\mathbf{e}}_3}\right)\right] \quad (14)$$

and $J_k(z_j)$ is a Bessel function of integer order k and argument $z_j=(\mathbf{d}\cdot\hat{\mathbf{e}}_j\varepsilon_j^0/\omega_j)$; the sum in Eq. (13) includes all (in practice appreciable) individual molecule-EMF couplings. Although Eq. (13) contains an infinite sum, the damped nature of the Bessel functions in Eq. (14), as a function of increasing order, generally ensures that lower-order multiphoton molecule-EMF couplings dominate the sum and the others can be neglected [4,10]. Since the Bessel functions are oscillatory in nature, increasing field strengths may actually decrease the molecule-EMF coupling.

From Eq. (10), the resonance ($\Delta=0$) period of the time-dependent excited-state population is

$$\tau=\frac{2\pi}{|\zeta(\delta_1,\delta_3)|_{\rm res}}, \quad (15)$$

where $|\zeta(\delta_1,\delta_3)|_{\rm res}$ is evaluated using Eq. (13) at the resonance value of ω_b. $\bar{P}_2(\delta_1,\delta_3)$, as a function of ω_b, represents the phase-dependent absorption spectrum or resonance profile for the two-level system in the HMR RWA. When $|\zeta(\delta_1,\delta_3)|$ is approximately constant over a resonance profile, the resonance profile has a full width at half maximum $\mathscr{F}$ of

$$\mathscr{F}=\frac{2|\zeta(\delta_1,\delta_3)|_{\rm res}}{N_b}. \quad (16)$$

In general, the HMR RWA is applicable if the overall phase-dependent molecule-EMF coupling $|\zeta(\delta_1,\delta_3)|$ is much less than the beat frequency ω_b [4].

For the case of explicit interest for the applications considered in Sec. III, i.e., simultaneous one- and three-photon excitation, the dominant individual couplings are $C(1,0)$ and

$C(0,3)$. Therefore, from Eq. (13), the magnitude of the HMR-RWA overall molecule-EMF coupling can be reduced to

$$|\zeta(\delta_1,\delta_3)| = [|C(1,0)|^2 + |C(0,3)|^2 + 2C(1,0)C(0,3)\cos\delta]^{1/2}. \quad (17)$$

When the HMR-RWA molecule-EMF couplings in Eq. (17) are replaced by their perturbative counterparts Eqs. (7) and (8), one obtains the perturbative expression for the overall molecule-EMF coupling that appears in Eq. (9), which can be written as $P_2(\delta_1,\delta_3,t) = (t^2/4)|\zeta(\delta_1,\delta_3)|^2$. Note that even though $J_0(z_i)$ in Eq. (14) represents a zero-photon transition, for sufficiently large field strengths it can greatly modify the molecule-EMF coupling as the field strength changes [4,5].

By expanding the HMR-RWA resonance result for the time-dependent population of state 2, Eq. (10) with $\Delta = 0$, in powers of t and retaining only terms through order $(t)^2$; then expanding $|\zeta(\delta_1,\delta_3)|^2$, by expansion of the Bessel functions $J_0(z)$, $J_3(z)$, and $J_1(z)$ in powers of z; and keeping terms through sixth overall order in the fields, the third-order perturbative result for the time-dependent population of state 2, Eq. (9), can be obtained, except for pure transition dipole terms above first order [i.e., the term μ^3 in Eq. (8)]. In general, as with the previously derived two-level molecular ($\mathbf{d}\neq\mathbf{0}$) one- and two-color RWA's, the HMR RWA fails in the limit that $\mathbf{d}=\mathbf{0}$ when it only supports one-photon transitions, i.e., the atomic RWA result corresponding to the absence of permanent dipole moments [1,4,5]. It is well known, even with $\mathbf{d}=\mathbf{0}$, that a two-level model can support all odd-photon, $N=1,3,5,7,\ldots$, transitions. It is necessary to utilize perturbative corrections [3] to the RWA, via the appropriate Floquet secular equation, in order to obtain reliable representations of the $N>2$ transition probabilities when $\mathbf{d}$ is ''small.'' Therefore, the HMR RWA will be most applicable when the permanent dipole mechanism is the dominant mechanism for a given $N>2$ multiphoton transition. For $N=1$ and 2, small-time and low-field expansions of the RWA results agree precisely with perturbation theory with $\mathbf{d}=\mathbf{0}$ or $\mathbf{d}\neq\mathbf{0}$ [10,28].

C. Numerical aspects

The validity of the HMR RWA can be investigated (see Sec. III and Ref. [10]) by comparison of the RWA results with exact calculations, which, of course, include all possible transition mechanisms. In the applications discussed here, the phase-dependent time-dependent populations and the phase-dependent long-time averaged (steady-state) populations of the molecular states are determined utilizing a Taylor-series method [29] and the Riemann product integral method [2,30–32], respectively, combined with the Floquet formalism [2,4,21–25], as discussed in detail by Kondo, Blokker, and Meath [4] and Brown and Meath [10]. Utilizing 540 Riemann intervals and 90 integration points, the steady-state populations generally converged to four or five significant figures. Using a step size of $2\pi/540$ and a nine-term Taylor series provides the evolution operators to 12-figure accuracy and thus the time-dependent populations to four or five significant figures for all times considered.

For molecular problems, it is often important to average transition probabilities and related observables, with respect to molecular orientations relative to the field directions [2,7,10,11,33–40]. Here free orientational averaging, where all orientations are equally probable, will be carried out; this corresponds to the situation where the absorbing molecules are randomly oriented with respect to the laser beams and/or to the classical limit of rotational averaging, which is more appropriate for heavy molecules or higher temperatures. The importance of orientational or rotational averaging has been demonstrated for both the one-color and two-color excitation of molecules [2,7,11,33–38], including the phase control of excitation processes [10,39,40]. Expressions for the free orientationally averaged time-dependent populations of molecular states, and the associated orientationally averaged resonance profiles, and discussions of their evaluation are available in the literature [10,33,34]. Using 72-point Gaussian quadrature to perform the angular integrations numerically, the steady-state and temporal populations generally converged to three or four figures.

III. RESULTS AND DISCUSSION

The explicit examples considered in this section involve the harmonic two-color simultaneous three- and one-photon excitations between two energy levels. The molecular parameters are given by $E_{21}=0.1$, $\mu=3.0$, and $d=6.5$. These parameters, which are representative of a two-level configuration in substituted aromatic molecules [41], have been used in harmonic two-color simultaneous two- and one-photon transition calculations [10] as well as other previous theoretical laser-molecule calculations [4,34,42,43]. In order to ascertain the role of permanent dipole moments in two-color phase-control problems, two cases must be considered: (a) optimization of phase control for $\mathbf{d}=\mathbf{0}$ and (b) optimization of phase control for $\mathbf{d}\neq\mathbf{0}$. Optimization of phase control involves, in part, choosing the field parameters so that the three-photon and the one-photon laser-molecule couplings are equal. Here the perturbation theory, Eqs. (7) and (8), or the HMR RWA, Eq. (14), expressions for the couplings are used for this purpose; a discussion of the usefulness of each for the problem of interest is contained in the following sections.

A. Optimization of phase control for $d=0$

Although the effects of $\mathbf{d}\neq\mathbf{0}$ on the dynamics and the resonance profiles arising from the interaction of one (or two) cw laser(s) with a molecule have been well demonstrated [1–11,27–29,33–35,42,43], few studies involving the control of molecular excitations have taken explicit account of the presence of permanent dipole moments. Therefore, we begin by choosing the field parameters in order to optimize phase control assuming $\mathbf{d}=\mathbf{0}$. If $\mathbf{d}=\mathbf{0}$, the perturbative results Eqs. (7) and (8) must be utilized in order to estimate the field strengths that will optimize phase control in the exact calculations; the RWA does not support three-photon excitations in this limit (see Sec. II B). The field strength for the one-photon transition is $\varepsilon_1^0 = 1\times10^{-6}$ (3.51×10^4 W/cm^2), while the field strength for the three-photon transition is $\varepsilon_3^0 = 1.255\times10^{-3}$ (5.527×10^{10} W/cm^2). These field strengths are chosen such that the laser-molecule couplings

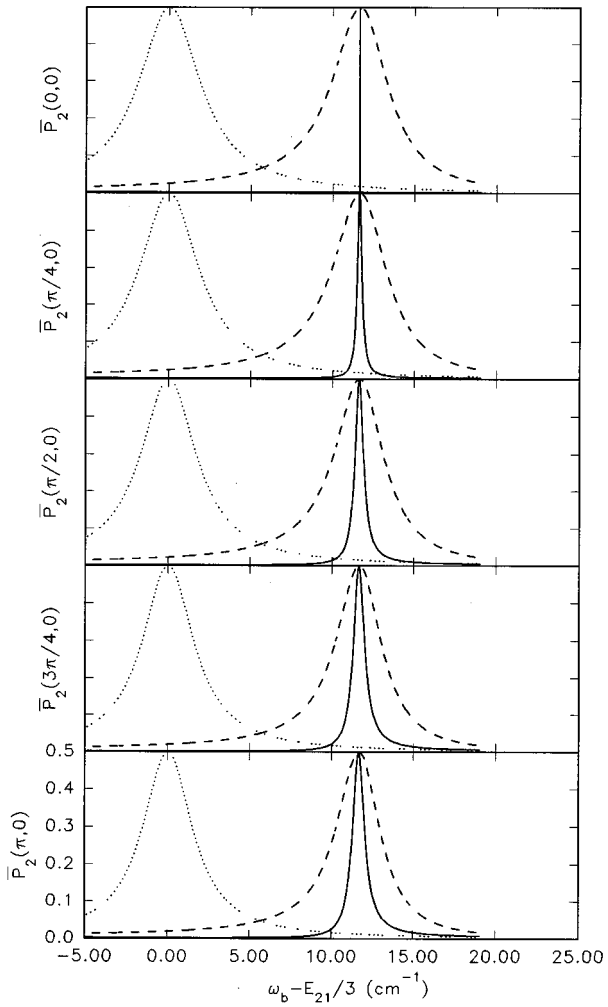

FIG. 1. Fixed molecule-EMF orientation ($\hat{\mathbf{e}}_1 \| \hat{\mathbf{e}}_3 \| \boldsymbol{\mu} \| \mathbf{d}$) resonance profiles, the long-time averaged population of the excited state $P_2(\delta_1, \delta_3)$ vs the beat frequency detuning ($\omega_b - E_{21}/3$), calculated in the HMR RWA ($\cdots$) and by exact Floquet methods, $d=0$ (—) and $d=6.5$ (----), for the simultaneous one- and three-photon two-color excitation of the model two-level molecule, as a function of the relative phase ($\delta_1 - 3\delta_3$) of the two lasers and with the field strengths $\varepsilon_3^0 = 1.255 \times 10^{-3}$ and $\varepsilon_1^0 = 1 \times 10^{-6}$ chosen to optimize control for $d=0$.

are of the same magnitude as those in our recent study of simultaneous two- and one-photon molecular excitation [10]. The transition and permanent dipole moments are taken to be aligned ($\boldsymbol{\mu} \| \mathbf{d}$) and the electric fields are taken to be parallel to each other and to the dipole moments $\hat{\mathbf{e}}_1 \| \hat{\mathbf{e}}_3 \| \boldsymbol{\mu} \| \mathbf{d}$. The field strengths are such that the magnitudes of the perturbative one-photon coupling Eq. (7) and of the perturbative three-photon coupling Eq. (8) are equal: $|[C(1)]_{\text{pert}}| = |[C(3)]_{\text{pert}}| \approx 3.000 \times 10^{-6}$. The sign of the three-photon coupling is the reverse of the one-photon couplings: $[C(1)]_{\text{pert}}$ is positive and $[C(3)]_{\text{pert}}$ is negative.

The resonance profiles are illustrated in Fig. 1 for various phases of the one-photon laser δ_1, with the phase of the three-photon laser δ_3 set to zero. Each part of the figure contains three curves: the resonance profile for $\mathbf{d}=\mathbf{0}$, the optimized phase control case calculated using the exact Floquet technique, and the resonance profiles for $|\mathbf{d}|=6.5$ calculated using the HMR RWA and by using the exact Floquet technique. We will begin with a discussion of the $\mathbf{d}=\mathbf{0}$ results and then discuss and contrast to the $\mathbf{d}\neq\mathbf{0}$ results.

The exact resonance profiles exhibit a two-color Bloch-Siegert shift of 11.6 cm^{-1} to higher frequency for all (δ_1, δ_3) combinations (see Fig. 1) relative to the perturbation theory or weak field resonance frequency of $\omega_b = 7315.667$ cm^{-1} [$\Delta=0$ in Eq. (12) with $N_1=1$, $N_3=3$, and $N_b=3$]. This shift is the same as that exhibited by the one-color three-photon resonance profile for the same field strength ($\varepsilon_3^0 = 1.255 \times 10^{-3}$); the analogous shift for the one-color one-photon resonance profile is insignificant. The Bloch-Siegert shift is very important since its magnitude is greater than the full widths at half maximum (FWHM's) of the resonance profiles for all (δ_1, δ_3) combinations. Therefore, if the weak-field resonance frequencies were assumed in the exact calculation, the resonances would be missed entirely. The Bloch-Siegert shift is much greater ($\sim$50 times larger) than the Bloch-Siegert shift for the analogous two- and one-photon excitation for the same molecule-EMF coupling strengths [10]. This agrees with the general trend for an increase in Bloch-Siegert shift with an increase in photonicity of a transition as was exhibited previously in the one-color case [3,33].

The $\mathbf{d}=\mathbf{0}$ results exhibit 99.99% phase control as the FWHM's vary from less than 0.001 cm^{-1} to 0.883 cm^{-1} as the relative phase $\delta = (\delta_1 - 3\delta_3)$ varies from 0 to π (see Fig. 1 and Table I). The percentage of phase control is defined as

$$(\%\ \text{control}) = \frac{\mathcal{F}_{\max} - \mathcal{F}_{\min}}{\mathcal{F}_{\max} + \mathcal{F}_{\min}}, \tag{18}$$

which is analogous to the definition based on the intensity of ionization signal used previously [16]. The FWHM's of the exact resonance profiles are in very good agreement with the predictions based on the perturbative molecule-EMF couplings and Eqs. (16) and (17); see Table I. The perturbative predictions are essentially within 0.6% of the exact results. This indicates the perturbative predictions for the molecule-EMF couplings are reliable even though perturbation theory cannot be used to obtain the long-time behavior of the populations of the molecular states or the associated resonance profiles. The reliability of perturbation theory in this regard is also seen in that control of the combined one- and three-photon transition is obtained in the exact calculations for the field strengths predicted via the perturbative molecule-EMF couplings.

Phase control is also reflected in the exact temporal calculations for $\mathbf{d}=\mathbf{0}$, which are carried out at the exact resonance frequency $(\omega_b^{\text{Floquet}})_{\text{res}} \approx 7327.33$ cm^{-1} for each relative phase [see Fig. 2, where $P_2(\delta_1, \delta_3, t)$ is shown for $\delta_1 - 3\delta_3 = 0, \pi/4, \pi/2, 3\pi/4, \pi$]. The period of the time-dependent population decreases from ''infinity'' since the molecule-EMF coupling increases from approximately zero as the relative phase goes from zero to π, which is a consequence of the inverse relationship between the temporal period and the molecule-EMF coupling; see Eq. (15). The periods are ''reliably'' predicted using the perturbatively calculated molecule-EMF coupling in Eq. (15).

We now consider the (real) $d=6.5$ molecule, bearing in mind that the field strengths were chosen to optimize phase

TABLE I. FWHM of the resonance profiles of Fig. 1 ($d=6.5$ or 0) as a function of the relative phase, $\delta=\delta_1-3\delta_3$ with $\delta_3=0$, of the two lasers. PT denotes perturbation theory calculations of the FWHM obtained using the perturbative molecule-EMF couplings, Eqs. (7) and (8), and Eqs. (16) and (17).

Calculation	Phase (δ)	FWHM (cm^{-1})	$[\omega_b]_{res}$ (cm^{-1})
HMR RWA	0	4.541	7315.667
Floquet ($d\neq 0$)		4.116	7327.327
PT ($d\neq 0$)		4.124	7315.667
Floquet ($d=0$)		<0.001	7327.321
PT ($d=0$)		<0.001	7315.667
HMR RWA	$\pi/4$	4.425	7315.667
Floquet ($d\neq 0$)		4.001	7327.330
PT ($d\neq 0$)		4.007	7315.667
Floquet ($d=0$)		0.338	7327.324
PT ($d=0$)		0.336	7315.667
HMR RWA	$\pi/2$	4.131	7315.667
Floquet ($d\neq 0$)		3.707	7327.338
PT ($d\neq 0$)		3.711	7315.667
Floquet ($d=0$)		0.624	7327.331
PT ($d=0$)		0.621	7315.667
HMR RWA	$3\pi/4$	3.815	7315.667
Floquet ($d\neq 0$)		3.387	7327.345
PT ($d\neq 0$)		3.389	7315.667
Floquet ($d=0$)		0.816	7327.337
PT ($d=0$)		0.811	7315.667
HMR RWA	π	3.676	7315.667
Floquet ($d\neq 0$)		3.246	7327.348
PT ($d\neq 0$)		3.246	7315.667
Floquet ($d=0$)		0.883	7327.340
PT ($d=0$)		0.878	7315.667

control for $\mathbf{d}=\mathbf{0}$. The $\mathbf{d}=\mathbf{0}$ optimized field strengths are such that for the $\mathbf{d}\neq\mathbf{0}$ molecule, the perturbative one-photon coupling and the perturbative three-photon coupling, as calculated using Eqs. (7) and (8), respectively, are no longer equal: $[C(1)]_{pert}\approx 3.000\times 10^{-6}$ and $[C(3)]_{pert}\approx 2.518\times 10^{-5}$ and furthermore $[C(3)]_{pert}$ is positive for $d=6.5$ versus negative when $\mathbf{d}=\mathbf{0}$. The ten-fold increase in the magnitude of the three-photon coupling with $\mathbf{d}\neq\mathbf{0}$ compared to $\mathbf{d}=\mathbf{0}$, as well as the change in sign of $[C(3)]_{pert}$, indicates that permanent dipoles have a pronounced effect in the three-photon transition.

The exact resonance profiles, calculated using Floquet methods, analogous to the $\mathbf{d}=\mathbf{0}$ results, but setting $d=6.5$ in the calculations, are included in Fig. 1. The choice of field strengths, chosen to optimize the phase control of the $\mathbf{d}=\mathbf{0}$ molecule, leads to little phase dependence in these resonance profiles and what is present is in the opposite sense to the $\mathbf{d}=\mathbf{0}$ case; that is, for $d=6.5$ the FWHM's of the profiles decrease with increasing $\delta=\delta_1-3\delta_3$; see also Table I. The lack of control [11.8% control based on Eq. (18)] for $d=6.5$ is also clear from the temporal plots of Fig. 2, where the period of the time-dependent population changes little

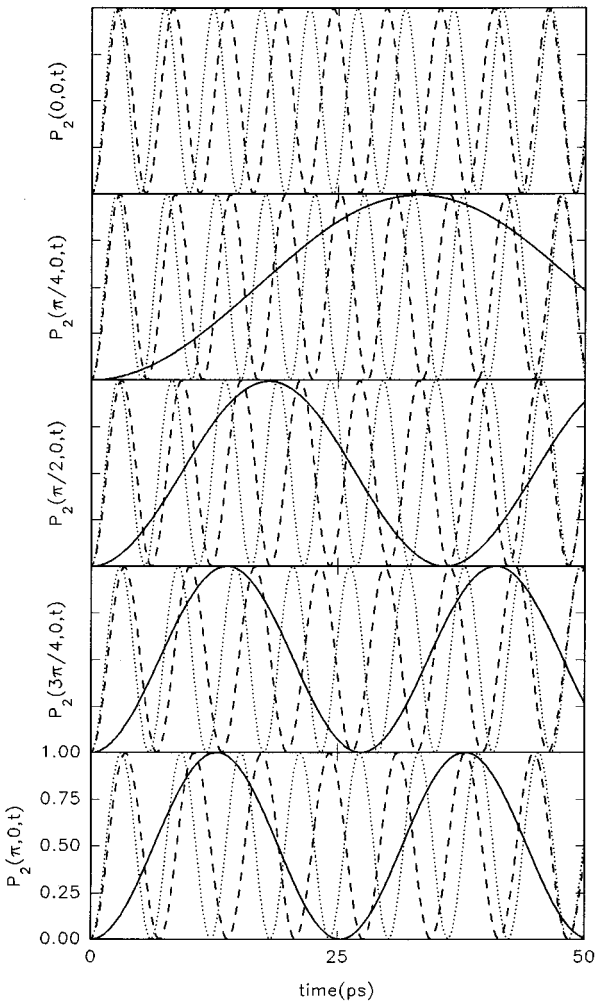

FIG. 2. Time-dependent population of the excited state 2, $P_2(\delta_1,\delta_3,t)$, calculated in the HMR RWA ($\cdots$) and by exact Floquet methods, $d=0$ (——) and $d=6.5$ (----), as a function of time and the relative phase of the two lasers, for the corresponding $\omega_b=\omega_b^{res}$ for each δ and for the field strengths chosen to optimize control for $d=0$. For $\delta=0$, $P_2(t)$ is essentially zero over the time scale shown for the exact $d=0$ Floquet results.

with δ. Relative to the $\mathbf{d}=\mathbf{0}$ results, for $d=6.5$ the three-photon excitation dominates the one-photon excitation process for all δ, since the three-photon coupling is approximately ten times larger than the one-photon molecule-EMF coupling. Phase control of the excitation process can be achieved for the $d=6.5$ molecule by proper selection of the laser fields (see Sec. III B).

As discussed previously, the FWHM's of the resonance profiles and hence the related periods of the temporal evolution of the excited state, for $\mathbf{d}=\mathbf{0}$, calculated using the perturbative expression for the molecule-EMF coupling and Eqs. (16) and (17), agree very closely with the exact Floquet results and this is also valid for $d=6.5$ where the perturbative and Floquet results for the FWHM agree to within 0.2%; see Table I. On the other hand, while the one-photon HMR-RWA molecule-EMF coupling $C(1,0)\approx 2.995\times 10^{-6}$ compares very well with the one-photon perturbative coupling $\approx 3.000\times 10^{-6}$, the three-photon HMR-RWA molecule-EMF coupling $C(0,3)\approx 2.808\times 10^{-5}$ is approximately 10% higher

than the perturbative three-photon molecule-EMF coupling $\approx 2.518\times10^{-5}$ since the HMR RWA does not include the μ^3 three-photon transition mechanism (see Sec. II B). Therefore, the FWHM's of the HMR-RWA resonance profiles ($d=6.5$) are larger than those determined from the exact calculations. This is illustrated in Fig. 1 (see also Table I), where the HMR-RWA resonance profiles can be compared with the exact results for $\mathbf{d}\neq\mathbf{0}$. As with the exact $\mathbf{d}\neq\mathbf{0}$ calculations, the HMR-RWA resonance profiles do not vary significantly with phase. Also, of course, the HMR-RWA profiles do not exhibit the Bloch-Siegert shifts seen in the exact resonance profiles.

If the Floquet and HMR-RWA temporal calculations for $d=6.5$ are carried out at their respective resonance frequencies $(\omega_b^{\text{Floquet}})_{\text{res}}\approx 7327.34\ \text{cm}^{-1}$ and $(\omega_b^{\text{WF}})_{\text{res}}=7315.667\ \text{cm}^{-1}$ (see Table I for the exact resonance frequency for each relative phase), the two sets of results for $P_2(\delta_1,\delta_3,t)$ are relatively independent of phase, but can differ significantly over the time scale shown for a given relative phase (see Fig. 2). This arises because the HMR-RWA three-photon coupling is larger than the correct result for all relative phases $\delta=(\delta_1-3\delta_3)$, which results in a reduced period in the RWA relative to the exact temporal behavior [see Eq. (15)]. Thus, for $t\sim 25$ ps, the RWA temporal behavior becomes completely out of phase with the exact results. For larger times the two sets of results can agree rather well, for example, for $t\sim 50$ ps, before again becoming out of phase with each other. This type of inversion of the temporal behavior of Floquet versus RWA results and its consequences in the interpretation of ir multiphoton excitation processes has been discussed previously [29,44]. If the exact temporal evolution of the excited state is computed for the weak-field resonance frequency $(\omega_b^{\text{WF}})_{\text{res}}=7315.667\ \text{cm}^{-1}$, that is neglecting the Bloch-Siegert shift, very large discrepancies between the exact and the HMR-RWA temporal results would be exhibited since the difference in resonance frequencies between the exact and the weak-field limits is much larger than the FWHM's of the resonance profiles for all relative phases δ. Thus the period of the exact temporal evolution for $\omega=(\omega_b^{\text{WF}})_{\text{res}}$ will be very large compared to HMR-RWA period for this frequency.

As discussed above, the HMR-RWA result for the three-photon coupling neglects the μ^3 contribution to the excitation mechanism and this causes disagreements between the RWA and the exact results. It is interesting to note that if RWA molecule-EMF couplings are replaced by the corresponding perturbatively determined couplings in the RWA analytical expressions for the resonance profile and the time-dependent population of the excited state, Eqs. (11) and (10), respectively, excellent agreement with the corresponding exact results will be obtained, aside from effects directly related to the absence of the Bloch-Siegert shift in the RWA calculation. This comment applies for both the $\mathbf{d}\neq\mathbf{0}$ and the $\mathbf{d}=\mathbf{0}$ sets of results. Thus, for example, if the time-dependent population of the excited state is calculated at the weak-field resonance frequency $\omega=(\omega_b^{\text{WF}})_{\text{res}}$, utilizing the HMR-RWA expression Eq. (10) but using the perturbative molecule-EMF couplings in place of the HMR-RWA couplings, the result will be indistinguishable from the exact calculations shown in Fig. 2.

B. Optimization of phase control for $d\neq 0$

When $\mathbf{d}\neq\mathbf{0}$, there is a choice of whether to utilize the perturbation theory or the HMR-RWA expressions for the molecule-EMF coupling to estimate the field strengths necessary to optimize phase control. Keeping the field strength for the laser driving the one-photon transition at the value used in Sec. III A, $\varepsilon_1^0=1\times10^{-6}$ ($3.51\times10^4\ \text{W/cm}^2$), the field strength for the three-photon transition must be changed to $\varepsilon_3^0=6.175\times10^{-4}$ ($1.338\times10^{10}\ \text{W/cm}^2$) in order to optimize phase control utilizing perturbation theory. These field strengths are such that the perturbative one-photon coupling Eq. (7) and the perturbative three-photon coupling Eq. (8) are equal: $[C(1)]_{\text{pert}}=[C(3)]_{\text{pert}}\approx 3.000\times10^{-6}$. Unlike when $\mathbf{d}=\mathbf{0}$, $[C(1)]_{\text{pert}}$ and $[C(3)]_{\text{pert}}$ both have positive values. Using the HMR RWA, the laser field strength for the one-photon transition is $\varepsilon_1^0=1\times10^{-6}$ ($3.51\times10^4\ \text{W/cm}^2$), while the field strength for the three-photon transition must be changed to $\varepsilon_3^0=6.000\times10^{-4}$ ($1.263\times10^{10}\ \text{W/cm}^2$). The field strengths are such that the HMR-RWA three-photon coupling $C(0,3)$ and the HMR-RWA one-photon coupling $C(1,0)$, as calculated using Eq. (14), are approximately equal: $C(0,3)\approx 3.077\times10^{-6}$ and $C(1,0)\approx 2.990\times10^{-6}$.

The resonance profiles are illustrated in Fig. 3 for various relative phases $\delta=(\delta_1-3\delta_3)$, with the phase of the three-photon laser δ_3 set to zero. Each part of the figure contains three curves: the exact resonance profile where the field strengths are chosen in order to optimize phase control using the perturbative molecule-EMF couplings Eqs. (7) and (8) and the exact and the HMR-RWA resonance profiles where phase control has been optimized using the HMR-RWA molecule-EMF coupling Eq. (14). The exact resonance profiles for the perturbatively chosen fields exhibit a two-color Bloch-Siegert shift of 2.8 cm^{-1} to higher frequency for all (δ_1,δ_3) combinations relative to the weak-field resonance frequency of $\omega_b=7315.667\ \text{cm}^{-1}$, while the exact resonance profiles for the HMR-RWA selected fields exhibit a two-color Bloch-Siegert shift of 2.7 cm^{-1} to higher frequency. These shifts are the same as those exhibited by the one-color three-photon resonance profiles for the same field strengths.

Phase control is exhibited for both sets of exact resonance profiles. The FWHM's for the exact profiles for the perturbatively chosen fields vary from 0.878 cm^{-1} for $\delta=0$ to less than 0.001 cm^{-1} for $\delta=\pi$, while for the HMR-RWA fields, they vary from 0.841 to 0.036 cm^{-1} as δ varies from 0 to π (see Table II): 99.8% and 91.8% control, respectively, based on Eq. (18). The phase control of the combined one- and three-photon transitions is more complete for the perturbatively chosen field strengths since, as discussed previously, the FWHM's of the exact resonance profiles generally agree very well with those calculated using the perturbative expression for the molecule-EMF coupling and Eqs. (16) and (17); see Table II. On the other hand, the exact resonance profiles for the HMR-RWA chosen fields do not exhibit as complete phase control since the HMR-RWA expression for the three-photon coupling, which neglects the μ^3 transition mechanism, underestimates the actual three-photon field strength needed to optimize control. Therefore, the FWHM's of the HMR-RWA resonance profiles are 5.6%, 5.5%, 5.5%, and 5.4% greater than those for the exact profiles for the

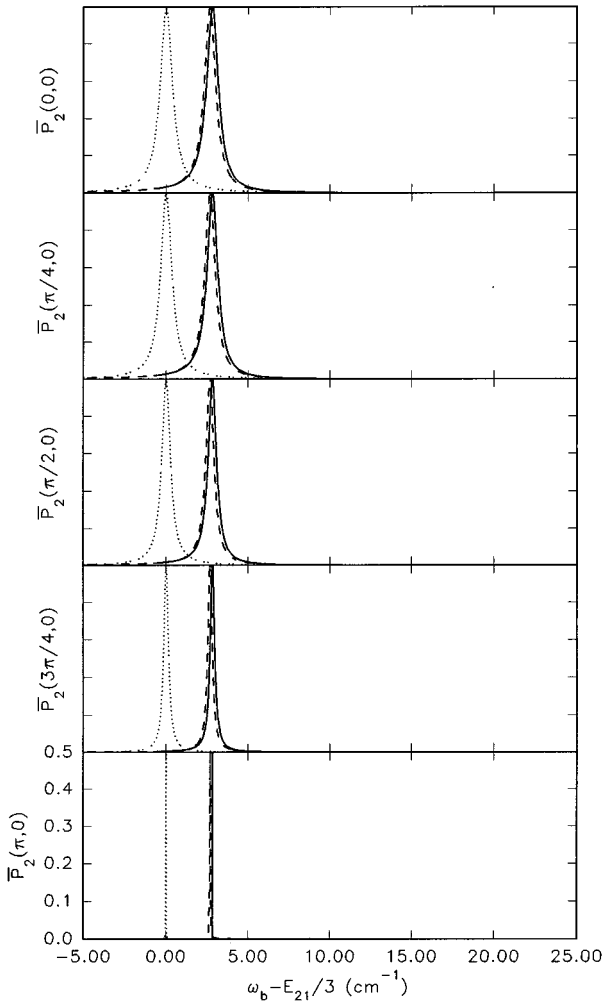

FIG. 3. Fixed molecule-EMF orientation ($\hat{\mathbf{e}}_1 \| \hat{\mathbf{e}}_3 \| \boldsymbol{\mu} \| \mathbf{d}$) resonance profiles, the long-time averaged population of the excited state $P_2(\delta_1, \delta_3)$ vs detuning ($\omega_b - E_{21}/3$), calculated by exact Floquet methods, for field strengths chosen to optimize control using perturbative couplings $\varepsilon_3^0 = 6.175 \times 10^{-4}$ and $\varepsilon_1^0 = 1 \times 10^{-6}$ (——), and by both exact Floquet methods (----) and in the HMR RWA ($\cdot \cdot \cdot \cdot$), for field strengths chosen to optimize control using HMR-RWA couplings $\varepsilon_3^0 = 6.000 \times 10^{-4}$ and $\varepsilon_1^0 = 1 \times 10^{-6}$, for the simultaneous one- and three-photon two-color excitation of the model ($d = 6.5$) two-level molecule, as a function of the relative phase ($\delta_1 - 3\delta_3$) of the two lasers.

HMR-RWA chosen fields as δ varies for 0 to $3\pi/4$, while for $\delta = \pi$ it is 64% smaller. On the other hand, utilizing the perturbative one- and three-photon couplings associated with the HMR-RWA optimized field strengths $[C(1)]_{\text{pert}} \approx 3.000 \times 10^{-6}$ and $[C(3)]_{\text{pert}} \approx 2.752 \times 10^{-6}$ and Eqs. (16) and (17), the FWHM's agree to within 0.3%.

The HMR-RWA resonance profiles are included in Fig. 3 and they exhibit ''complete'' phase control for the optimal laser fields based on the HMR-RWA laser-molecule couplings; in the calculations reported here, these fields were not completely optimized in the RWA, that is, $C(0,3) \approx 3.077 \times 10^{-6}$ and $C(1,0) \approx 2.990 \times 10^{-6}$. Of course, the Bloch-Siegert shifts, present in the exact Floquet results, are absent in all RWA calculations. Aside from this and their $\sim 6\%$ too large FWHM's, the HMR-RWA resonance profiles model well the exact results. The modeling can be improved, as discussed in Sec. III A, by simply replacing the HMR-RWA molecule-laser couplings by the perturbative couplings estimated for optimal combined one- and three-photon transition control. The resonance profiles obtained this way will be graphically indistinguishable from the exact results once the profiles are frequency normalized for the Bloch-Siegert shift.

TABLE II. FWHM of the resonance profiles of Fig. 3 ($d = 6.5$) as a function of the relative phase, $\delta_1 - 3\delta_3$ with $\delta_3 = 0$, of the two lasers. Floquet (RWA) indicates that the exact calculations were performed using the HMR-RWA selected fields, while Floquet (PT) indicates that the perturbative fields were used. PT and PT (RWA) indicate using the perturbatively and the HMR-RWA selected control fields, respectively, in the calculation of the FWHM's using Eqs. (7), (8), (16), and (17).

Calculation	Phase (δ)	FWHM (cm^{-1})	$[\omega_b]_{\text{res}}$ (cm^{-1})
HMR RWA	0	0.888	7315.667
Floquet (RWA)		0.841	7318.329
PT (RWA)		0.842	7315.667
Floquet (PT)		0.878	7318.486
PT		0.878	7315.667
HMR RWA	$\pi/4$	0.820	7315.667
Floquet (RWA)		0.777	7318.330
PT (RWA)		0.778	7315.667
Floquet (PT)		0.810	7318.488
PT		0.811	7315.667
HMR RWA	$\pi/2$	0.628	7315.667
Floquet (RWA)		0.595	7318.334
PT (RWA)		0.596	7315.667
Floquet (PT)		0.621	7318.492
PT		0.621	7315.667
HMR RWA	$3\pi/4$	0.340	7315.667
Floquet (RWA)		0.323	7318.337
PT (RWA)		0.324	7315.667
Floquet (PT)		0.336	7318.495
PT		0.336	7315.667
HMR RWA	π	0.013	7315.667
Floquet (RWA)		0.036	7318.338
PT (RWA)		0.036	7315.667
Floquet (PT)		0.001	7318.497
PT		<0.001	7315.667

Phase control is exhibited in the exact temporal calculations for $\mathbf{d} \neq \mathbf{0}$, which are carried out at the exact resonance frequency for each relative phase for both the perturbatively chosen fields, $(\omega_b^{\text{Floquet PT}})_{\text{res}} \approx 7318.49$ cm^{-1}, and for the HMR-RWA selected fields, $(\omega_b^{\text{Floquet RWA}})_{\text{res}} \approx 7318.33$ cm^{-1}; see Fig. 4. For both sets of calculations, phase control is in the opposite sense to the $\mathbf{d} = \mathbf{0}$ results of Sec. III A, that is, the period of the time-dependent population increases, since the molecule-EMF coupling decreases, as the relative phase changes from zero to π. The phase control is in the opposite sense for the two calculations because the three-photon cou-

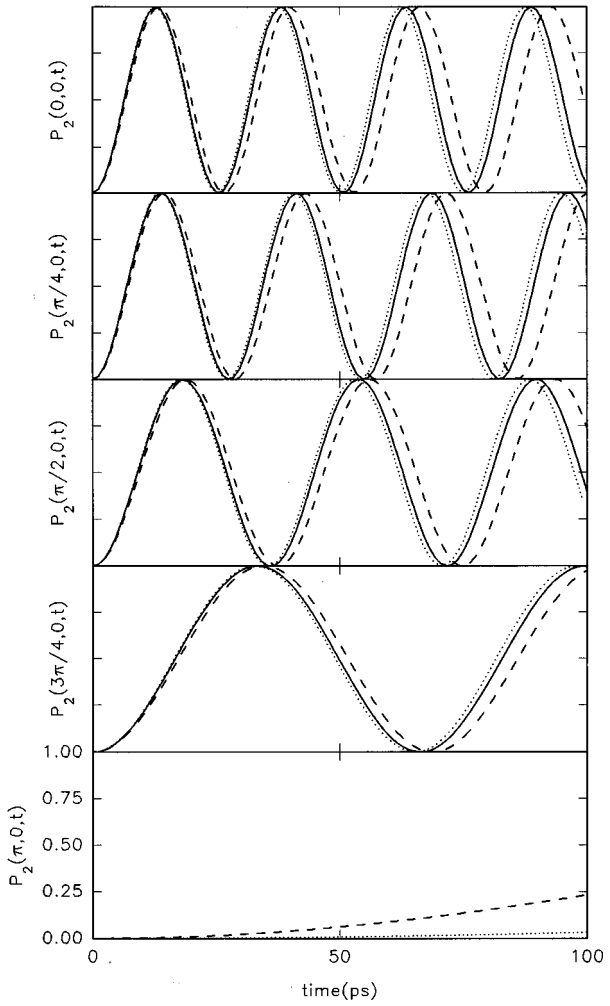

FIG. 4. Time-dependent population of the excited state 2, $P_2(\delta_1,\delta_3,t)$ for the model ($d=6.5$) two-level molecule, calculated by exact Floquet methods, for field strengths chosen to optimize control using perturbative couplings (——), and by both exact Floquet methods (----) and in the HMR RWA ($\cdots$), for field strengths chosen to optimize control using HMR-RWA couplings, as a function of time and the relative phase of the two lasers, for the corresponding $\omega_b=\omega_b^{\rm res}$ for each δ. For $\delta=\pi$, $P_2(t)$ is essentially zero over the time scale shown for the field strengths for optimal control estimated by perturbation theory.

pling is positive versus negative and therefore the sign of the interference term in Eq. (17) changes, for $d=6.5$ versus $\mathbf{d}=\mathbf{0}$. Using either the perturbatively or the HMR-RWA chosen field strengths in the perturbative molecule-EMF couplings in Eqs. (15) and (17), the respective periods of temporal evolution are ''reliably'' predicted. The perturbatively chosen fields give more complete control and temporally this is best seen for $\delta=\pi$, where the period is much greater than for the HMR-RWA selected fields. Over the time scale depicted, the HMR RWA yields reasonable predictions of the exact temporal behavior, although the periods for all δ are slightly too small (a reflection of the couplings being approximately 6% too large). However, over sufficiently longer time scales, the HMR-RWA temporal behavior will become completely out of phase with the exact results (see Sec. III A and Refs. [10,29,44]).

In the examples just discussed, the permanent dipole mechanism, that is, the term in Eq. (8) of the form $d^2\mu$, tends to dominate the transition dipole mechanism (the term of the form μ^3) in the total three-photon molecule-EMF coupling. Thus, for example, in the exact Floquet calculations, phase control is more or less obtained if either perturbation theory or the HMR RWA is used to estimate the optimal fields for control of the simultaneous one- and three-photon excitation process. For the model molecule studied, the difference between the permanent dipoles of the states involved in the transition, $d=6.5$, is quite large compared to the transition dipole, $\mu=3$. Often d and μ can be of more comparable sizes.

C. Optimization of phase control for $d\neq 0$ ($d=2.5$)

In order to more clearly understand the possible effects of permanent dipoles in the phase control of molecular excitation processes, we now consider a model where $d\approx\mu$. For this purpose we consider a ''pseudomolecule'' with the same molecular parameters as before except $d=2.5$. The laser field strength for the one-photon transition is kept at the $d=6.5$ value; $\varepsilon_1^0=1\times10^{-6}$ (3.51×10^4 W/cm^2) for both the perturbative and HMR-RWA choices of optimal control field strengths. In order that the perturbative one- and three-photon couplings are equal for $d=2.5$, again at $[C(1)]_{\rm pert}=[C(3)]_{\rm pert}\approx3.000\times10^{-6}$, the field strength for the three-photon transition must be increased to $\varepsilon_3^0=1.719\times10^{-3}$ (1.037×10^{11} W/cm^2) from 6.175×10^{-4} (1.338×10^{10} W/cm^2) for $d=6.5$. Using the HMR-RWA couplings, the field driving the three-photon transition must be increased from 6.000×10^{-4} (1.263×10^{10} W/cm^2) to $\varepsilon_3^0=1.120\times10^{-3}$ (4.402×10^{10} W/cm^2), so that the three-photon coupling $C(0,3)\approx2.962\times10^{-6}$ is approximately equal to the one-photon coupling $C(1,0)\approx2.995\times10^{-6}$.

For all relative phases $\delta=(\delta_1-3\delta_3)$, the exact resonance profiles for the perturbatively chosen fields exhibit a two-color Bloch-Siegert shift of 21.9 cm^{-1} to higher frequency relative to the weak-field resonance frequency of $(\omega_b^{\rm WF})_{\rm res}=7315.667$ cm^{-1}, while the exact resonance profiles for the HMR-RWA selected fields exhibit a two-color Bloch-Siegert shift of 9.3 cm^{-1}; see Fig. 5 and Table III. The Bloch-Siegert shifts for the two-color process are the same as those exhibited by the one-color three-photon resonance profiles for the same field strengths and therefore the large difference in Bloch-Siegert shifts between the perturbatively and HMR-RWA chosen fields profiles is due to the difference in the three-photon field strengths for the two calculations (1.719×10^{-3} versus 1.120×10^{-3}, respectively). Unlike for $d=6.5$ (Fig. 3), there is no overlap between the resonance profiles for the perturbatively and the HMR-RWA chosen fields. The profiles overlap for $d=6.5$ because the three-photon field strengths are much more similar, $\varepsilon_3^0=6.175\times10^{-4}$ (1.338×10^{10} W/cm^2) for perturbatively chosen fields and $\varepsilon_3^0=6.000\times10^{-4}$ (1.263×10^{10} W/cm^2) for the HMR-RWA chosen fields, relative to the corresponding fields for $d=2.5$.

The FWHM's for the exact resonance profiles for the perturbatively chosen fields vary from 0.878 to 0.010 cm^{-1}, 97.8% control, while for the HMR-RWA fields they vary from 0.562 to 0.320 cm^{-1}, 27.4% control, as δ varies from

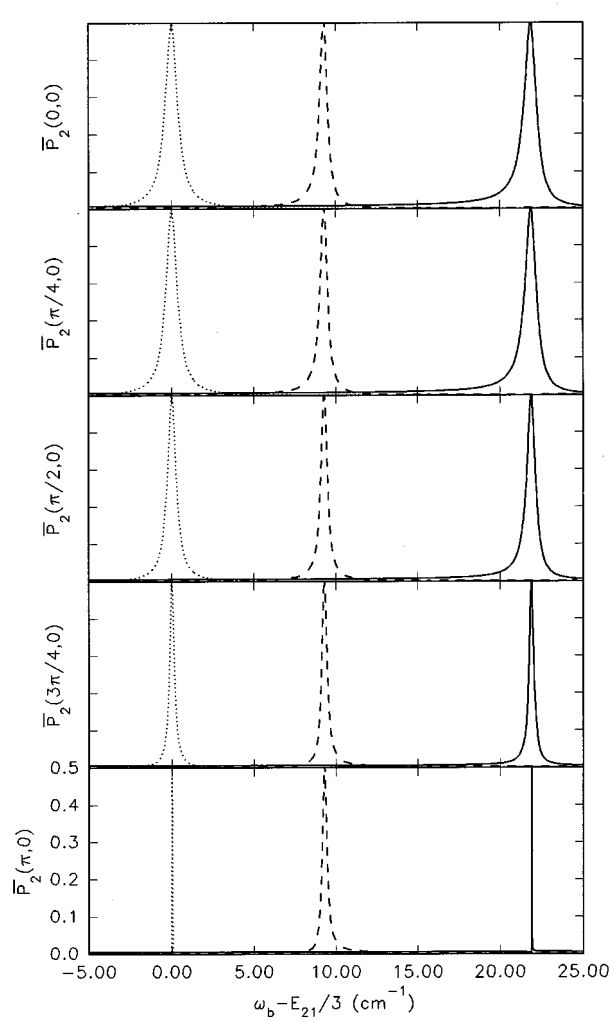

FIG. 5. Fixed molecule-EMF orientation ($\hat{\mathbf{e}}_1 \| \hat{\mathbf{e}}_3 \| \boldsymbol{\mu} \| \mathbf{d}$) resonance profiles, the long-time averaged population of the excited state $P_2(\delta_1, \delta_3)$ vs the beat frequency detuning ($\omega_b - E_{21}/3$), calculated by exact Floquet methods, for field strengths chosen to optimize control using perturbative couplings $\varepsilon_3^0 = 1.719 \times 10^{-3}$ and $\varepsilon_1^0 = 1 \times 10^{-6}$ (——), and by both exact Floquet methods (----) and in the HMR RWA ($\cdots$), for field strengths chosen to optimize control using HMR-RWA couplings $\varepsilon_3^0 = 1.120 \times 10^{-3}$ and $\varepsilon_1^0 = 1 \times 10^{-6}$, for the simultaneous one- and three-photon two-color excitation of the model ($d = 2.5$) two-level molecule, as a function of the relative phase ($\delta_1 - 3\delta_3$) of the two lasers.

0 to π, respectively; see Table III. Almost complete phase control is exhibited for the perturbatively chosen field strengths, but these results do not exhibit as much phase control (99.8%) as when $d = 6.5$.

Compared to the $d = 6.5$ molecule, the FWHM's for the exact resonance profiles for the HMR-RWA selected fields agree poorly with those for the HMR-RWA calculations since the neglected μ^3 transition mechanism is now much more dominant in the three-photon molecule-EMF coupling. Therefore, although the HMR-RWA one-photon coupling $C(1,0) \approx 2.995 \times 10^{-6}$ agrees very well with the perturbative one-photon coupling $[C(1)]_{\text{pert}} \approx 3.000 \times 10^{-6}$, the HMR-RWA three-photon coupling $C\ (0,3) \approx 2.962 \times 10^{-6}$ is much larger than the perturbative three-photon coupling $[C(3)]_{\text{pert}} \approx 8.298 \times 10^{-7}$, for the HMR-RWA chosen fields.

TABLE III. FWHM of the resonance profiles of Fig. 5 ($d = 2.5$) as a function of the relative phase, $\delta_1 - 3\delta_3$ with $\delta_3 = 0$, of the two lasers. Floquet (RWA) indicates that the exact calculations were performed using the HMR-RWA fields, while Floquet (PT) indicates that the perturbative fields were used. PT and PT (RWA) indicate using the perturbatively and the HMR-RWA selected control fields, respectively, in the calculation of the FWHM's using Eqs. (7), (8), (16), and (17).

Calculation	Phase (δ)	FWHM (cm^{-1})	$[\omega_b]_{\text{res}}$ (cm^{-1})
HMR RWA	0	0.872	7315.667
Floquet (RWA)		0.562	7324.950
PT (RWA)		0.560	7315.667
Floquet (PT)		0.878	7337.541
PT		0.878	7315.667
HMR RWA	$\pi/4$	0.805	7315.667
Floquet (RWA)		0.533	7324.952
PT (RWA)		0.532	7315.667
Floquet (PT)		0.812	7337.545
PT		0.811	7315.667
HMR RWA	$\pi/2$	0.616	7315.667
Floquet (RWA)		0.456	7324.958
PT (RWA)		0.455	7315.667
Floquet (PT)		0.619	7337.554
PT		0.621	7315.667
HMR RWA	$3\pi/4$	0.334	7315.667
Floquet (RWA)		0.364	7324.965
PT (RWA)		0.363	7315.667
Floquet (PT)		0.334	7337.565
PT		0.336	7315.667
HMR RWA	π	0.005	7315.667
Floquet (RWA)		0.320	7324.967
PT (RWA)		0.318	7315.667
Floquet (PT)		0.010	7337.568
PT		<0.001	7315.667

Hence the FWHM's calculated in the HMR RWA are much larger for the positive ($\delta = 0, \pi/4$) and zero ($\delta = \pi/2$) interference profiles [the interference term in Eq. (17) is positive] and much smaller for the negative ($\delta = 3\pi/4, \pi$) interference profiles than those for the exact calculations based on the RWA selected three-photon field strength; see Table III. However, the FWHM's of the exact resonance profiles for the HMR-RWA selected field strengths agree, within 0.6%, to the results calculated using the perturbative molecule-EMF couplings and Eqs. (16) and (17) and these field strengths. Since the HMR RWA incorrectly predicts the optimum control three-photon molecule-EMF coupling, the exact resonance profiles for the HMR-RWA selected fields exhibit little phase control (27.4%).

Since the period of the temporal evolution of the excited state is related to the FWHM of the resonance profiles via Eqs. (15) and (16), the exact temporal behavior (not shown explicitly here) of the excited state for the perturbatively chosen field strengths carried out at the exact resonance fre-

quency $(\omega_b^{\text{Floquet PT}})_{\text{res}} \approx 7337.55\ \text{cm}^{-1}$ will exhibit essentially complete phase control. Conversely, for the HMR-RWA selected field strengths, the exact temporal behavior carried out at the exact resonance frequency $(\omega_b^{\text{Floquet RWA}})_{\text{res}} \approx 7324.96\ \text{cm}^{-1}$ will exhibit little phase control. Thus, for $d=2.5$ ($d \approx \mu$) and for the field strengths considered here, the perturbatively chosen field strengths provide control while the HMR-RWA selected fields do not provide adequate results for the three-photon molecule-EMF coupling and therefore little control is exhibited in either the exact resonance profiles or the associated exact temporal behavior. In contrast, for $d=6.5$ ($d \gg \mu$), either the perturbatively chosen or the HMR-RWA selected field strengths provide almost complete phase control.

D. Optimization of phase control for $d=0$ ("real" $d=2.5$)

For comparison purposes, let us consider the $\mathbf{d}=\mathbf{0}$ calculations, analogous to those of Sec. III A for $d=6.5$, for the pseudomolecule with $d=2.5$. Since the field strengths are to be chosen assuming the perturbative one- and three-photon couplings are the same for $\mathbf{d}=\mathbf{0}$, they are the same as those in Sec. III A, i.e., for the one-photon transition $\varepsilon_1^0=1\times10^{-6}$ (3.51×10^4 W/cm^2) and for the three-photon transition $\varepsilon_3^0=1.255\times10^{-3}$ (5.527×10^{10} W/cm^2). Exact resonance profiles for $\mathbf{d}=\mathbf{0}$ and analogous results for $d=2.5$ as a function of relative phase are illustrated in Fig. 6. While the $\mathbf{d}=\mathbf{0}$ results exhibit phase control (99.99%) (see the discussion in Sec. III A and Table I), the analogous $d=2.5$ results exhibit less phase control (38.5%) as the FWHM's vary from 0.612 to 0.272 cm^{-1} as δ varies from 0 to π and the phase control that is exhibited is in the opposite sense to that for $\mathbf{d}=\mathbf{0}$; compare Tables IV and I. The exact ($d=2.5$) FWHM's are greater than those for $\mathbf{d}=\mathbf{0}$ for $\delta=0$ and $\pi/4$ while they are smaller for $\delta=\pi/2$, $3\pi/4$, and π [see Fig. 6, Tables IV ($d=2.5$) and I ($d=0$)]; for $d=6.5$ (see Fig. 1 and Table I) the FWHM's are greater for all relative phases. The exact FWHM's for $d=2.5$ are reliably predicted from the overall perturbative molecule-EMF coupling and Eq. (16). When $d=2.5$, the perturbative three-photon coupling $[C(3)]_{\text{pert}} \approx 1.167\times10^{-6}$ is of the same magnitude as the one-photon coupling $[C(1)]_{\text{pert}} \approx 3.000\ \times10^{-6}$ and therefore, if one assumes $\mathbf{d}=\mathbf{0}$, when, in fact, $d=2.5$, there is still 38.5% control, based on Eq. (18). Conversely, for $d=6.5$, the three-photon coupling $[C(3)]_{\text{pert}} \approx 2.518\times10^{-5}$ is approximately ten times larger than the one-photon coupling and there is only 11.8% control (see Sec. III A).

The behavior of the FWHM's for the exact resonance profiles for $d=2.5$ relative to $\mathbf{d}=\mathbf{0}$ is also reflected in the temporal calculations, where are carried out at the exact resonance frequency for each relative phase $(\omega_b^{\text{Floquet}})_{\text{res}} \approx 7327.33\ \text{cm}^{-1}$ (see Fig. 7). As the relative phase varies from zero to π, the period of the time-dependent population increases from 33 to 80 ps when $d=2.5$, while it decreases from infinity to 25 ps for $\mathbf{d}=\mathbf{0}$ since the field strengths have been chosen to optimize phase control for $\mathbf{d}=\mathbf{0}$. The period for $d=2.5$ is shorter than that for $\mathbf{d}=\mathbf{0}$ for $\delta=0$ and $\pi/4$ while it is longer for $\delta=\pi/2$, $3\pi/4$, and π. However, for $d=2.5$ neither the longest period is as long nor the shortest period as short as that for $\mathbf{d}=\mathbf{0}$, so obviously there is less

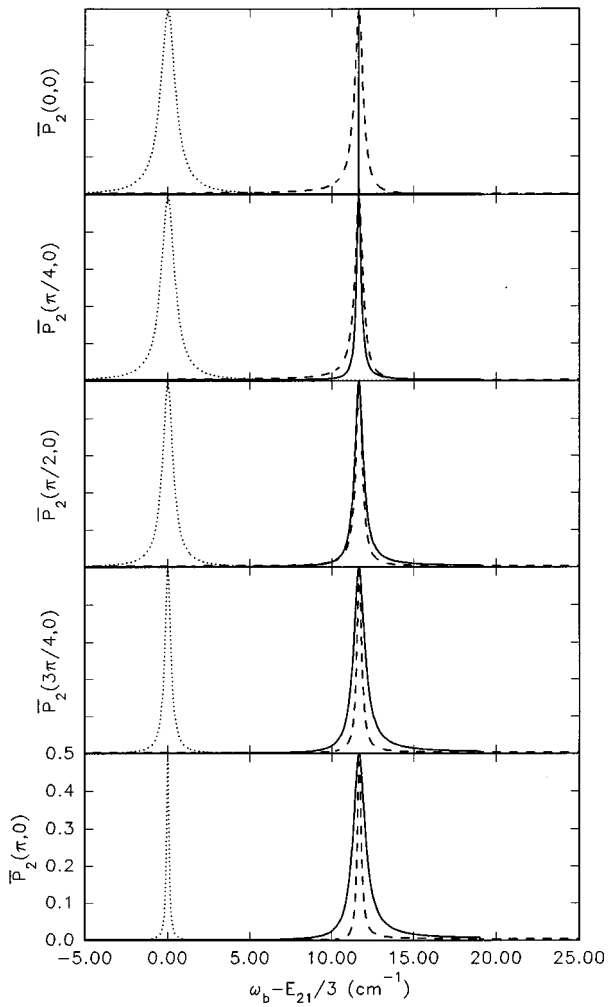

FIG. 6. Fixed molecule-EMF orientation ($\hat{\mathbf{e}}_1 \| \hat{\mathbf{e}}_3 \| \boldsymbol{\mu} \| \mathbf{d}$) resonance profiles, the long-time averaged population of the excited state $P_2(\delta_1, \delta_3)$ vs the beat frequency detuning ($\omega_b - E_{21}/3$) calculated in the HMR RWA ($\cdots$) and by exact Floquet methods, $d=0$ (——) and $d=2.5$ (----), for the simultaneous one- and three-photon two-color excitation of the model two-level molecule, as a function of the relative phase ($\delta_1 - 3\delta_3$) of the two lasers and with the field strengths $\varepsilon_3^0=1.255\times10^{-3}$ and $\varepsilon_1^0=1\times10^{-6}$ chosen to optimize control for $d=0$.

temporal phase control when $d=2.5$. When $d=6.5$, the period of the temporal behavior of the excited state is shorter for all relative phases (see Fig. 2). Thus, as is reflected both temporally and in the associated resonance profiles, neglecting the permanent dipole moments in determining the field strengths for optimal control will inevitably lead to a loss of control, although the exact amount of control lost depends upon the relative values of d and μ.

E. Orientational averaging

Only one example, where phase control has been optimized for the fixed orientation $\hat{\mathbf{e}}_1 \| \hat{\mathbf{e}}_3 \| \boldsymbol{\mu} \| \mathbf{d}$ when $d=6.5$ (see Sec. III B), will be considered since it will illustrate the main effects of orientational averaging for the harmonic simultaneous three- and one-photon excitation. Orientationally averaged temporal behavior and associated resonance profiles are

TABLE IV. FWHM of the resonance profiles of Fig. 6 ($d=2.5$ or 0; see Table I for $d=0$ results) as a function of the relative phase, $\delta=\delta_1-3\delta_3$ with $\delta_3=0$, of the two lasers. PT denotes perturbation theory calculations of the FWHM obtained using the perturbative molecule-EMF couplings, Eqs. (7) and (8), and Eqs. (16) and (17).

Calculation	Phase (δ)	FWHM (cm^{-1})	$[\omega_b]_{res}$ (cm^{-1})
HMR RWA	0	1.047	7315.667
Floquet ($d\neq 0$)		0.612	7327.324
PT ($d\neq 0$)		0.610	7315.667
HMR RWA	$\pi/4$	0.970	7315.667
Floquet ($d\neq 0$)		0.575	7327.326
PT ($d\neq 0$)		0.573	7315.667
HMR RWA	$\pi/2$	0.751	7315.667
Floquet ($d\neq 0$)		0.472	7327.333
PT ($d\neq 0$)		0.471	7315.667
HMR RWA	$3\pi/4$	0.432	7315.667
Floquet ($d\neq 0$)		0.342	7327.340
PT ($d\neq 0$)		0.340	7315.667
HMR RWA	π	0.171	7315.667
Floquet ($d\neq 0$)		0.272	7327.344
PT ($d\neq 0$)		0.268	7315.667

characteristic of molecules randomly situated in the gas or solution phase rather than with a specific orientation relative to the laser fields.

The free orientationally averaged [10,33,34] perturbatively determined temporal behavior is given by

$$\begin{aligned} P_2^{\rm rot}(\delta,t) &= \frac{t^2}{8}\int_0^{\pi}\{[C(1)]_{\rm pert}^2\cos^2\beta+[C(3)]_{\rm pert}^2\cos^6\beta \\ &\quad +2[C(1)]_{\rm pert}[C(3)]_{\rm pert}\cos^4\beta\,\cos\delta\}\sin\beta\,d\beta \\ &= \frac{t^2}{4}\{\tfrac{1}{3}[C(1)]_{\rm pert}^2+\tfrac{1}{7}[C(3)]_{\rm pert}^2 \\ &\quad +\tfrac{2}{5}[C(1)]_{\rm pert}[C(3)]_{\rm pert}\cos\delta\} \\ &= \frac{t^2}{4}[\zeta_{\rm av}^{\rm pert}(\delta_1,\delta_3)]^2 \end{aligned} \tag{19}$$

where here the molecule-EMF couplings $[C(1)]_{\rm pert}$ and $[C(3)]_{\rm pert}$ now depend only on the magnitudes of the permanent and transition dipole moments since the angular dependence on β (the angle between the fields and the dipoles) has been factored out; see Eqs. (7) and (8). There is an obvious loss of phase control if one uses the fixed orientation optimal control field strengths since the orientationally averaged overall molecule-EMF coupling in Eq. (19), $\zeta_{\rm av}^{\rm pert}(\delta_1,\delta_3)$, no longer approaches zero as the relative phase δ approaches π. In fact, if the one- and three-photon molecule-EMF couplings are set equal, $[C(1)]_{\rm pert}=[C(3)]_{\rm pert}=C$, as done for the fixed orientation problem (Sec. III B), the minimum value of the overall molecule-EMF coupling that can be obtained is $(8/105)^{1/2}C$ compared to a maximum value of $(92/105)^{1/2}C$. However, if the orientationally averaged molecule-EMF coupling is utilized to maximize control, i.e., to minimize $|\zeta_{\rm av}^{\rm pert}(\pi,0)|$, the new relationship between the one- and three-photon coupling is $1.4[C(1)]_{\rm pert}=[C(3)]_{\rm pert}$. Using this result, the minimum value of the overall molecule-EMF coupling that can be obtained is $(4/75)^{1/2}[C(1)]_{\rm pert}$ as compared to a maximum value of $(88/75)^{1/2}[C(1)]_{\rm pert}$. Based on the orientationally "optimized" control, the new three-photon field strength is $\varepsilon_3^0=6.908\times10^{-4}$ (1.675×10^{10} W/cm^2) when the one-photon field strength is fixed at the value used in Sec. III B, $\varepsilon_1^0=1.000\times10^{-6}$ (3.51×10^4 W/cm^2).

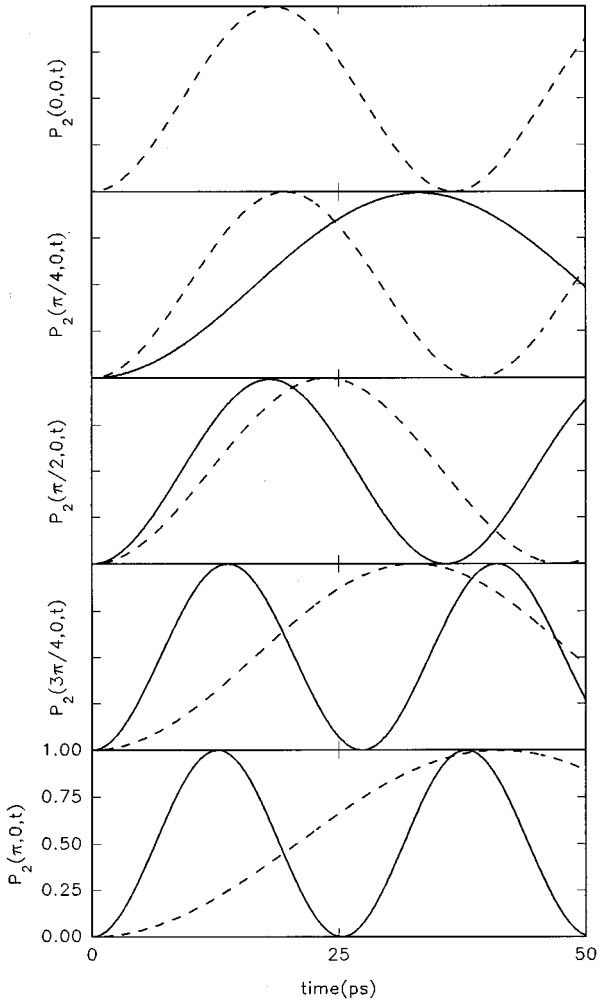

FIG. 7. Time-dependent population of the excited state 2, $\bar{P}_2(\delta_1,\delta_3,t)$ calculated by exact Floquet methods, $d=0$ (——) and $d=2.5$ (----), as a function of time and the relative phase of the two lasers, for the corresponding $\omega_b=\omega_b^{\rm res}$ for each δ and for the field strengths chosen to optimize control for $d=0$. For $\delta=0$, $P_2(t)$ is essentially zero over the time scale shown for the exact $d=0$ Floquet results.

The orientationally averaged resonance profiles $\bar{P}_2^{\rm rot}(\delta_1,\delta_3)$ versus $(\omega_b-E_{21}/3)$ calculated using the perturbative overall molecule-EMF coupling in the HMR-RWA expression Eq. (11) and by using the exact methods are illustrated in Fig. 8 for the parallel fixed orientation optimized

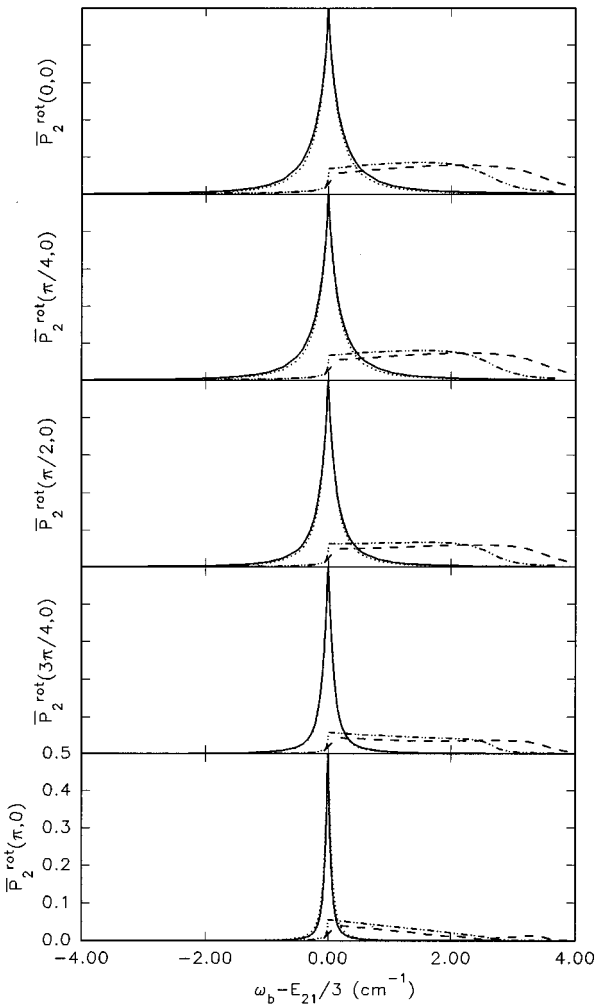

FIG. 8. Orientational averaged resonance profiles, the orientationally averaged long-time averaged population of the excited state $\bar{P}_2^{\rm rot}(\delta_1,\delta_3)$ vs beat frequency detuning $(\omega_b - E_{21}/3)$, for the $d=6.5$ parallel configuration optimal control field strengths $\varepsilon_3^0=6.175\times10^{-4}$ and $\varepsilon_1^0=1\times10^{-6}$, calculated in the HMR RWA $(\cdots)$ and by exact Floquet methods $(-\cdots-\cdots)$ and for the orientationally "optimized" field strenghts $\varepsilon_3^0=6.908\times10^{-4}$ and $\varepsilon_1^0=1\times10^{-6}$ calculated in the HMR RWA (——) and by exact Floquet methods (----), as a function of the relative phase of the two lasers. In the HMR-RWA calculations the RWA molecule-EMF couplings are replaced by the appropriate perturbative molecule-EMF couplings (see the main text).

field strengths (Sec. III B) $\varepsilon_1^0=1.000\times10^{-6}$ $(3.509\times10^4$ W/cm$^2)$ and $\varepsilon_3^0=6.175\times10^{-4}$ $(1.338\times10^{10}$ W/cm$^2)$ and for the orientationally averaged optimized field strengths. The orientationally averaged resonance profiles are very dissimilar to their fixed orientation $\hat{\mathbf{e}}_1\|\hat{\mathbf{e}}_3\|\boldsymbol{\mu}\|\mathbf{d}$ counterparts (see Fig. 3). We begin with a discussion of the exact resonance profiles and then follow with a discussion within the HMR RWA (using the perturbative overall molecule-EMF coupling, however).

Upon orientational averaging, many fixed molecule-laser configurations contribute to the resonance profile and the exact resonance frequencies vary considerably [33], corresponding to Bloch-Siegert shifts of 2.6 cm^{-1} (for $\hat{\mathbf{e}}_1\|\hat{\mathbf{e}}_3\|\boldsymbol{\mu}\|\mathbf{d}$) to zero (for $\hat{\mathbf{e}}_1\|\hat{\mathbf{e}}_3\perp\boldsymbol{\mu}\|\mathbf{d}$) and, further, the Bloch-Siegert shifts can often be larger than the FWHM's of the corresponding fixed configuration resonance profiles. Thus, in contradistinction to the simultaneous two- and one-photon excitation situation discussed previously [10], where the maximum Bloch-Siegert shift was small, 0.2 cm^{-1}, the orientationally averaged exact resonance profiles shown in Fig. 8 are "smeared out" over a large frequency range and therefore no resonance frequency can be defined that corresponds to a "maximum" in the resonance profile [33]. On the other hand, the HMR-RWA orientationally averaged profiles do not exhibit the same behavior since the HMR RWA does not include Bloch Siegert shifts and therefore the resonance frequencies, for all molecule-laser configurations contributing to the orientationally averaged resonance profile, are the same.

Although the exact orientationally averaged resonance profiles exhibit phase dependence, their corresponding exact temporal populations are not discussed further since they are extremely low: $P_2^{\rm rot}(\delta_1,\delta_3,t)<0.01$ for all relative phases over the time scale shown in Fig. 9. This behavior agrees with the fact that the resonance profile, at a given ω_b, is the long-time average of the temporal behavior of the excited-state population for that ω_b and all the exact orientationally averaged resonance profiles have small heights [e.g., maximum $\bar{P}_2^{\rm rot}(\delta_1,0)\approx0.08$]. Therefore, in what follows, we will consider the HMR-RWA temporal results, which will illustrate some effects of orientational averaging on the dynamics of the system in the absence of Bloch-Siegert shift effects.

The FWHM's for the HMR-RWA resonance profiles for the parallel configuration optimal control fields vary from 0.248 to 0.100 cm^{-1}, 42.5% control, while for the orientationally optimized fields they vary from 0.270 to 0.082 cm^{-1}, 53.4% control, as δ varies from 0 to π, respectively. Therefore, by optimizing the laser fields using the orientationally averaged expression for the overall perturbative molecule-EMF coupling, one can achieve a 10% increase in control within the HMR RWA.

The orientationally averaged temporal population of the excited state, for various relative phases, evaluated using the HMR RWA with the perturbative couplings, with the frequency set at the weak field resonance frequency $\omega_b=(\omega_b^{\rm WF})_{\rm res}=7315.667$ cm^{-1}, for the parallel orientation optimized field strengths and for the orientationally optimized field strengths are illustrated in Fig. 9. For the short-time behavior in the HMR RWA, a slight increase in control can be seen for the orientationally "optimized" field strengths relative to the parallel configuration case. However, over the time scale of the figure, for $\delta=0$, $\pi/4$, and $\pi/2$, the longer-time behavior becomes relatively independent of phase. This behavior is very similar to the recently studied orientationally averaged temporal behavior for the simultaneous two- and one-photon excitation. In contrast to the two- versus one-photon competition behavior, where phase control is lost for all phases, the three- versus one-photon temporal behavior shows more significant phase dependence for $\delta=3\pi/4$ and π (over the scale of the figure). If the orientational average (again with $\hat{\mathbf{e}}_1\|\hat{\mathbf{e}}_2$ and $\boldsymbol{\mu}\|\mathbf{d}$) of the perturbative temporal behavior [10] for the simultaneous one- and two-photon excitation is considered,

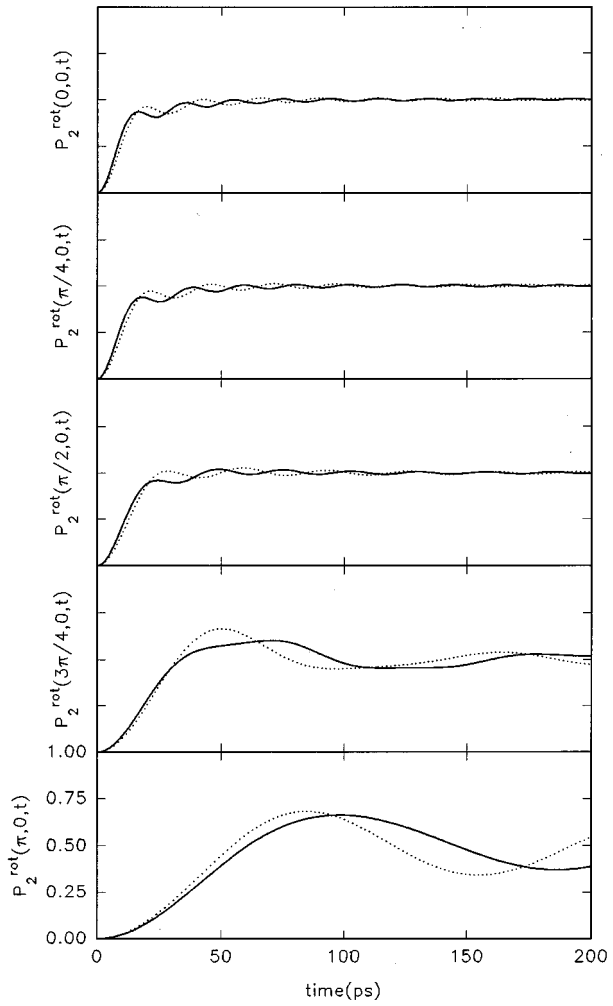

FIG. 9. Orientationally averaged HMR-RWA time-dependent populations of the excited state 2, $P_2^{\rm rot}(\delta_1,\delta_3,t)$, for the $d=6.5$ parallel configuration field strengths $\varepsilon_3^0=6.175\times10^{-4}$ and $\varepsilon_1^0=1\times10^{-6}$ ($\cdots$) and for the orientationally ''optimized'' field strengths $\varepsilon_3^0=6.908\times10^{-4}$ and $\varepsilon_1^0=1\times10^{-6}$ (——), as a function of time and the relative phase of the two lasers, for $\omega_b=(\omega_b^{\rm WF})_{\rm res}$.

$$P_2^{\rm rot}(\delta,t)=\frac{t^2}{4}\left\{\frac{1}{3}[C(1)]^2_{\rm pert}+\frac{1}{5}[C(2)]^2_{\rm pert}\right\}, \qquad (20)$$

the interference term averages out to zero and thus the orientationally averaged results are independent of phase in the perturbative approximation in contrast to the phase dependence occurring in the analogous three- versus one-photon result of Eq. (19).

IV. CONCLUDING REMARKS

A nonzero difference **d** in the permanent dipole moments between two molecular states involved in a two-color transition, involving simultaneous single- and multiphoton transitions, can have significant effects, relative to $\mathbf{d}=\mathbf{0}$, on the control of the state populations through the variation of the relative phase of the two lasers inducing the transitions. In this paper a two-level molecular model is used to investigate the effects of $\mathbf{d}\neq\mathbf{0}$, in this context, for the simultaneous one- and three-photon excitation of the ground state. In contrast to simultaneous one- and two-photon excitation [10], where $\mathbf{d}\neq\mathbf{0}$ is required for the two-photon transition to occur, competition between the one- and three-photon excitations can occur both when $\mathbf{d}=\mathbf{0}$ and when $\mathbf{d}\neq\mathbf{0}$. The control of excitation, that is, of the population of the excited state, is investigated both for a fixed laser-molecule orientation ($\hat{\mathbf{e}}_1\|\hat{\mathbf{e}}_3\|\boldsymbol{\mu}\|\mathbf{d}$) and for situations where the absorbing molecules are randomly orientated with respect to the laser field directions. The effects of the relative phase of the two lasers are discussed using both the temporal evolution of the excited-state population and the resonance profiles associated with the one- and three-photon simultaneous excitation process to monitor the effects of phase control.

For the fixed molecule-laser orientation studies, the role of permanent dipoles is investigated by choosing the laser fields to optimize phase control both with and without taking explicit account of the permanent dipoles when choosing the optimal field strengths. Sections III A and III B investigate phase control for a ''giant dipole'' molecule where $d\gg\mu$ ($d=6.5$ and $\mu=3$). Using the field strengths that lead to 100% phase control assuming $\mathbf{d}=\mathbf{0}$ yields little phase control in the ''real'' $d=6.5$ molecule. Keeping the one-photon field strength fixed, phase control can be achieved by markedly reducing the laser field strength associated with the three-photon molecule-EMF coupling so that the one- and three-photon couplings, including the effects of permanent dipoles, are equal in magnitude. Relative to $\mathbf{d}=\mathbf{0}$, the three-photon coupling $C(3)$ changes sign when $d=6.5$ since $C(3)\propto(2d^2-\mu^2)\mu$, that is, the permanent dipole and the pure transition dipole three-photon transition mechanisms contribute to the three-photon coupling in opposite senses. Thus the phase control changes ''sense'' as a function of the relative phase δ for $d=6.5$ relative to $\mathbf{d}=\mathbf{0}$; for example, the population of the excited state is maximized (minimized) for $\delta=\pi$ (0) versus $\delta=0$ (π) for $\mathbf{d}=\mathbf{0}$ and 6.5, respectively. Often d and μ are of more equal magnitude and the phase control of simultaneous one- and three-photon excitation in this situation is considered in Secs. III C and III D, where $d=2.5$ and $\mu=3$. In this example, relative to $\mathbf{d}=\mathbf{0}$, the three-photon laser field strength must be increased significantly to obtain phase control.

In these calculations reliable estimates for the optimal choices for the field strengths for phase control were provided by time-dependent perturbation theory predictions for the required molecule-EMF couplings even through perturbation theory results for the time dependence of the populations of the molecular states cannot be used for long times or to obtain resonance profiles. Indeed the RWA result for the three-photon coupling $[C(0,3)]\propto2d^2\mu$ neglects an important term ($-\mu^3$) relative to the more reliable perturbation theory expression $[C(3)]_{\rm pert}\propto(2d^2-\mu^2)\mu$. Thus, in the choice of laser field strengths for optimal phase control only the perturbation theory molecule-EMF couplings could be employed when $\mathbf{d}=\mathbf{0}$, whereas for $d=6.5$ and 2.5 the RWA couplings were also tested. When $d=6.5$ ($2d^2\mu\gg\mu^3$) the optimal control field strengths predicted by the RWA lead to almost complete control of the excited-state population while for $d=2.5$ ($2d^2\mu\sim\mu^3$) the corresponding RWA predictions are not at all reliable. In general, the correct analytical tools must be used to help estimate the field strengths for optimal

control of the excitation process and while perturbation theory performed well in the examples considered here, it will fail for more intense laser fields (larger molecule-EMF couplings).

The HMR RWA was also used to model the exact Floquet calculations of the temporal behavior of the molecular states and the related resonance profiles, for $\mathbf{d}\neq\mathbf{0}$. When the optimal control laser fields are chosen using the RWA, complete phase control of the excited state is achieved within the RWA. For common field strengths, the HMR-RWA calculations model well the exact calculations except for effects related to the absence of the two-color Bloch-Siegert shift in the resonance frequency in the RWA results. Discrepancies can also arise because of disagreements between the three-photon molecule-EMF couplings in the RWA versus the exact calculations. These affect the FWHM's of the resonance profiles and the period of the temporal evolution of the excited state, and while they are small for $d=6.5$ $(2d^2\mu\gg\mu^3)$, they are more significant for $d=2.5$ $(2d^2\mu\sim\mu^3)$. These non-Bloch-Siegert effects, in all the $\mathbf{d}\neq\mathbf{0}$ calculations, can be removed by replacing the RWA molecule-EMF couplings by the perturbative expressions for the couplings (at the same laser field strengths) in the HMR-RWA analytical expressions for the resonance profiles and the time-dependent populations of the molecular states. It should be emphasized that the effects of the Bloch-Siegert shift are important. Very often these are larger than the FWHM of the resonance profiles and therefore if the weak-field resonance frequency is assumed in the laser excitation process, as would occur in both the RWA and perturbation theory analyses of the problem, the resonances can be missed completely. However, once these shifts are taken into account, the analytical HMR-RWA expressions, augmented by the perturbative molecule-EMF couplings, can be very effective in analytically and reliably representing the phase control of molecular excitations for the laser-molecule couplings of the magnitude studied in this paper, without recourse to exact Floquet calculations.

The control of the combined one- and three-photon excitation process, for the situation where the absorbing molecules are randomly orientated with respect to the laser field directions, is discussed in Sec. III E. Since the molecule-EMF couplings required for control change with relative molecule-field orientations, effective control of the excitation process is lost relative to the fixed molecule-EMF configuration examples discussed earlier. Upon orientational averaging, both the temporal evolution of the excited-state populations and the resonance profiles show little dependence on the relative phase of the lasers. However, in agreement with the predictions of time-dependent perturbation theory, the phase dependence for the one- and three-photon competition studied here is more significant than that for the previously studied [10] one- and two-photon simultaneous excitation process. When random orientational averaging effects become important, the loss of phase control is inevitable in such competitive excitation processes. However, such phase control is observable in rotationally resolved excitation schemes [14–19].

The phase control of molecular excited-state populations, through two-color laser excitation and the interference between two optical excitation paths to the same final state, is a problem of considerable interest [12–19]. The magnitude of the interference is related to the relevant molecule-EMF couplings for the competing transitions and to the relative phase of the two lasers controlling the excitation paths. However, until recently, little explicit attention has been given to the effects of permanent dipoles and to those associated with the random orientation of the absorbing species in phase control studies. As illustrated here, for two-level dipolar molecular models, these effects are important in such problems since they both influence molecule-EMF couplings.

ACKNOWLEDGMENTS

This research was supported by a grant from the Natural Sciences and Engineering Research Council of Canada. A.B. would like to thank the Natural Sciences and Engineering Research Council of Canada for financial support.

[1] M. A. Kmetic and W. J. Meath, Phys. Lett. **108A**, 340 (1985).
[2] W. J. Meath, R. A. Thuraisingham, and M. A. Kmetic, Adv. Chem. Phys. **73**, 307 (1989).
[3] M. A. Kmetic and W. J. Meath, Phys. Rev. A **41**, 1556 (1990).
[4] A. E. Kondo, V. M. Blokker, and W. J. Meath, J. Chem. Phys. **96**, 2544 (1992).
[5] A. E. Kondo, W. J. Meath, S. Nilar, and A. J. Thakkar, Chem. Phys. **186**, 375 (1994).
[6] B. Dick and G. Hohlneicher, J. Chem. Phys. **76**, 5755 (1982).
[7] W. J. Meath and E. A. Power, J. Phys. B **17**, 763 (1984).
[8] D. L. Andrews and W. J. Meath, J. Phys. B **26**, 4133 (1993).
[9] M. Garcia-Sucre, E. Squitieri, J. L. Pas, and V. Mujica, J. Phys. B **27**, 4945 (1994).
[10] A. Brown and W. J. Meath, Chem. Phys. **198**, 91 (1995).
[11] B. N. Jagatap, W. J. Meath, D. Tittelbach-Helmrich, and R. P. Steer, J. Chem. Phys. **103**, 121 (1995).
[12] P. Brumer and M. Shapiro, Acc. Chem. Res. **22**, 407 (1988).
[13] P. Brumer and M. Shapiro, Annu. Rev. Phys. Chem. **43**, 257 (1992).
[14] M. Shapiro, J. W. Hepburn, and P. Brumer, Chem. Phys. Lett. **149**, 451 (1988).
[15] Z. Chen. P. Brumer, and M. Shapiro, J. Chem. Phys. **98**, 6843 (1993).
[16] S.-P. Lu, S. M. Park, Y. Xie, and R. J. Gordon, J. Chem. Phys. **96**, 6613 (1992).
[17] S. M. Park, S.-P. Lu, and R. J. Gordon, J. Chem. Phys. **94**, 8622 (1991).
[18] S.-P. Lu, S. M. Park, Y. Xie, and R. J. Gordon, in *Coherence Phenomena in Atoms and Molecules in Laser Fields*, edited by A. D. Bandrauk and S. C. Wallace (Plenum, New York, 1992), p. 303.
[19] V. D. Kleiman, L. Zhu, X. Li, and R. J. Gordon, J. Chem. Phys. **102**, 5863 (1995).
[20] P. W. Langhoff, S. T. Epstein, and M. Karplus, Rev. Mod. Phys. **44**, 602 (1972).

[21] J. H. Shirley, Phys. Rev. B **138**, 979 (1965).
[22] D. R. Dion and J. O. Hirschfelder, Adv. Chem. Phys. **35**, 265 (1976).
[23] J. V. Moloney and W. J. Meath, Mol. Phys. **31**, 1537 (1976); **30**, 171 (1975); **35**, 1163 (1978); J. Phys. B **11**, 2641 (1978).
[24] W. R. Salzman, Phys. Rev. **10**, 461 (1974); **16**, 1552 (1977); M. D. Burrows and W. R. Salzman, *ibid.* **15**, 1636 (1977).
[25] T. S. Ho and S. I. Chu, J. Phys. B **17**, 2101 (1984).
[26] T. S. Ho, S. I. Chu, and J. V. Tietz, Chem. Phys. Lett. **96**, 464 (1983).
[27] A. E. Kondo and W. J. Meath (unpublished).
[28] A. E. Kondo and W. J. Meath, J. Mol. Struct. (Theochem.) **232**, 23 (1991).
[29] S. Nakai and W. J. Meath, J. Chem. Phys. **96**, 4991 (1992).
[30] G. F. Thomas and W. J. Meath, J. Phys. B **16**, 951 (1983).
[31] R. B. Walker and R. K. Preston, J. Chem. Phys. **67**, 2017 (1977).
[32] E. P. Dougherty, Jr., S. D. Augustin, and H. Rabitz, J. Chem. Phys. **74**, 1175 (1981).
[33] R. A. Thuraisingham and W. J. Meath, Mol. Phys. **56**, 193 (1985).
[34] M. A. Kmetic, R. A. Thuraisingham, and W. J. Meath, Phys. Rev. A **33**, 1688 (1988).
[35] W. J. Meath and R. A. Thuraisingham, in *Atomic and Molecular Processes with Short Intense Laser Pulses*, edited by A. D. Bandrauk (Plenum, New York, 1988), p. 453.
[36] P. Tran, W. J. Meath, B. D. Wagner, and R. P. Steer, J. Chem. Phys. **100**, 4165 (1994).
[37] S. Chelkowski and A. D. Bandrauk, J. Chem. Phys. **99**, 4279 (1993).
[38] E. E. Aubanel, A. Conjusteau, and A. D. Bandrauk, Phys. Rev. A **48**, 4011 (1993).
[39] C. Asaro, P. Brumer, and M. Shapiro, Phys. Rev. Lett. **60**, 1634 (1988).
[40] C. K. Chan, P. Brumer, and M. Shapiro, J. Chem. Phys. **94**, 2688 (1991).
[41] W. Liptay, in *Excited States*, edited by E. C. Lim (Academic, New York, 1974), Vol. 1, p. 198.
[42] Y. B. Band, R. Bavli, and D. F. Heller, Chem. Phys. Lett. **156**, 405 (1989).
[43] R. Bavli, D. F. Heller, and Y. B. Band, Phys. Rev. A **41**, 3960 (1990).
[44] S. Nakai and W. J. Meath, Chem. Phys. **154**, 349 (1991).